2024 Tenth Indian Control Conference (ICC)
9 - 11 December, 2024
IISER Bhopal, India

Stability Analysis Using Describing Function For Non-Linear Attitude Control Loop with Slosh Dynamics of Chandrayaan-3 Landing Mission

Aditya R[1], Debajyoti Chakrabarti[2], Nivriti Priyadarshini[3], MP Rijesh[4], and GVP Bharat Kumar[5]

Abstract— **Chandrayaan-3 became the first Indian Lunar Lander mission which landed on Moon's south pole in 2023. The lunar landing mission consists of multiple phases where primary deceleration was done using liquid engines. The navigation, guidance, and control system dictates the trajectory and descent operations. Guidance generates the attitude reference profile to be tracked by the inner control loop. Attitude control is performed using non-linear reaction control system which operates in on-off mode. A high-fidelity mechanical analogous slosh (pendulum) model is used to analyze the sloshing phenomena and control stability during the powered descent phase. Propellant sloshing induces disturbance which can interact with the inner attitude control loop and impact the overall stability margins. The pulse width pulse frequency modulator (PWPFM) converts the linear control commands to non-linear on-off pulses for the reaction control system (RCS). PWPFM is the non-linear element present in the attitude control loop which will also impact the stability margins and introduce limit cycles. In this paper, the linear stability analysis of the attitude control loop with propellant slosh dynamics is extended to incorporate the PWPFM non-linearity using the describing function analysis. An algorithm to numerically compute describing function is proposed which resolves the initialization issue with integrators. The stability margins and stability of limit cycle as a function of time has been computed. Finally, a correlation between frequency domain analyses and high-fidelity time domain simulation is presented.**

I. INTRODUCTION

Chandrayaan-3 lander successfully soft-landed on the lunar surface on 23rd August 2023, embarking historical moment to perform first-ever soft landing near the south pole. Chandrayaan-3 is configured as a two-module system comprising of a Propulsion Module (PM) and a Lander Module (LM). The Chandrayaan-3 Integrated module was launched using GSLV-MK-III to Earth Parking Orbit (170 x 36400 km). The propulsion Module places the composite module in a 100 km lunar circular orbit after several earth- and moon-bound maneuvers. Lander gets separated in a 100 km lunar circular orbit post to which it performs a De-boost maneuver thereby reducing the orbit size from 100 km circular to 100 km x 30 km elliptical orbit.

At perilune (30 km) powered descent is initiated to perform a soft landing on the lunar surface. Lander is equipped with 4 throttleable engines rating 800 N each to perform powered descent operation and 8 Nos of 58 N Reaction Control System (RCS) thrusters to perform attitude control. Navigation, Guidance, and Control system facilitates the descent of the lander to the identified safe landing site on the lunar surface. Detailed powered descent trajectory is shown in Fig. 1. The primary objective of attitude control system during the powered descent phase is to track the guidance-generated reference attitude with the required accuracy.

Lander carries large propellant tanks for thrusting during the powered descent phase. Propellant gets consumed over the period. As the propellant gets depleted, the effect of liquid sloshing becomes more and more prominent. Sloshing motion can add instability to the attitude control system, which must be studied thoroughly to ascertain its impact on the attitude control system and stability margins. Various models available in the literature use a mechanical equivalence to represent the sloshing motion of propellant inside tanks. For instance, [1] suggests using a spring mass damper system to compute the sloshing forces and torques acting on spacecraft. The mass attached to the spring represents the sloshing mass while the spring constant is used to model the sloshing frequency. [2] suggests using a pendulum model wherein bob mass represents the sloshing mass and pendulum length along with the vehicle acceleration decides the frequency. Mechanical equivalence of all these models can be easily established. Here we have used the pendulum model to represent the slosh dynamics.

Attitude control for the lander is performed using 8 Nos of 58N rated RCS. The attitude control law is linear however the actuator operates in a non-linear on-off mode. Here a PWPF modulator is used to convert linear control commands to non-linear on-off pulses. The introduction of a non-linear element in the control loop will result in limit cycle behavior. Our previous work [3] details the slosh model derivation and linear stability analysis for a typical landing mission. In this paper, the linear stability analysis done in [3] is extended to non-linear stability analysis considering the PW-PFM non-linearity. [4] describes the analytical computation of describing function for standard non-linearities. [5] uses a similar approach for the numerical computation of describing function, however, it did not address the initialization issue for integrators. This paper proposes an improved numerical approach to derive the describing function of PWPFM. Moreover, the stability of limit cycles is evaluated using the extended Nyquist criteria. The stability analysis results are corroborated with the time domain simulation to bring out the attitude control performance during powered descent phase.

*This work is supported by U R Rao Satellite Centre(URSC), Indian Space Research Organization (ISRO),Bangalore 560017, India

[1]Aditya R, [2]Debajyoti Chakrabarti, and [4]MP Rijesh are Scientist/Engineer under the Control and Digital Area, URSC, adityar@ursc.gov.in, debjyoti.isro@gmail.com, & rijesh@ursc.gov.in

[3]Nivriti Priyadarshini and [5]GVP Bharat Kumar are Division Heads under the Control and Digital Area, URSC, nivriti@ursc.gov.in, & bharat@ursc.gov.in

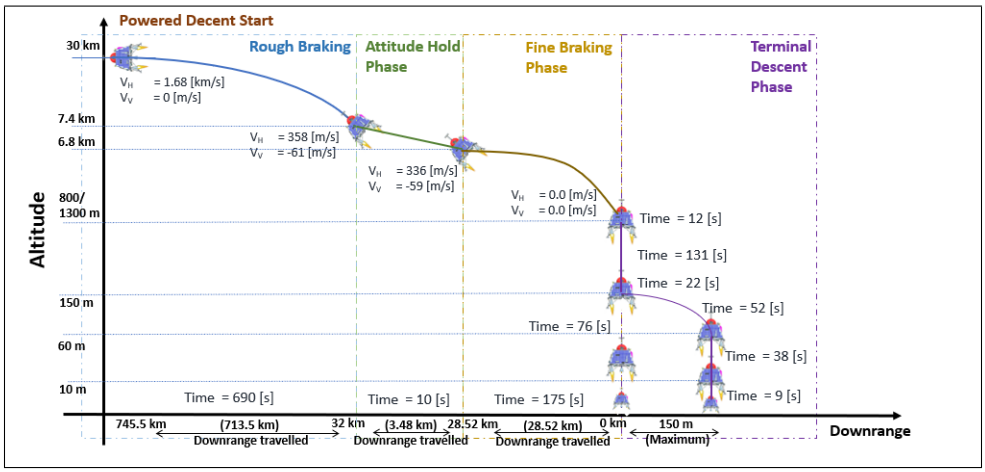


Fig. 1: Chandrayaan-3 Lander Powered Descent Trajectory

II. Lander Attitude Kinematics and Dynamics with Propellant Sloshing

A. Kinematics

The lander attitude kinematics can be represented in many ways. Using quaternion, attitude kinematics can be defined by (1).

$$\dot{q} = \frac{1}{2}\Omega(\omega)q \tag{1}$$

Where, q represents the spacecraft attitude with respect to a fixed inertial space. $\Omega(\omega)$ is given by,

$$\Omega(\omega) = \begin{bmatrix} 0 & \omega_z & -\omega_y & \omega_x \\ -\omega_z & 0 & \omega_x & \omega_y \\ \omega_y & -\omega_x & 0 & \omega_z \\ -\omega_x & -\omega_y & -\omega_z & 0 \end{bmatrix} \tag{2}$$

B. Lander Attitude Dynamics

Spacecraft dynamics follows the classical Euler moment equation. Dynamics of spacecraft with RCS, Liquid Engines, and propellant sloshing (refer [1]) can be described by (3).

$$I\dot{\omega} + \omega\dot{I} + \omega \times I\omega = \tau_{RCS} + \tau_{engine} + \tau_{slosh} \tag{3}$$

where, I is the spacecraft moment-of-inertia tensor, ω represents the angular velocity of lander with respect to inertial space, expressed in body frame ($\omega = [\omega_x, \omega_y, \omega_z]^T$), $\dot{\omega}$ represents the angular acceleration of lander, τ_{RCS} is the control moment generated by RCS, τ_{engine} is the disturbing moment due to engines and τ_{slosh} is the disturbing moment due to propellant sloshing.

C. Propellant Slosh Dynamics

The formulation of the slosh model consists of two segments: analogous pendulum dynamics (representing slosh phenomena) and disturbance torque emulating the effect of sloshing on spacecraft. The dynamic nature of the propellant participating in slosh is captured in terms of time-varying analogous pendulum parameters. The pendulum dynamics is formulated based on time derivative in the Newtonian frame of reference i.e. inertial frame of reference (refer [3] for complete derivation).

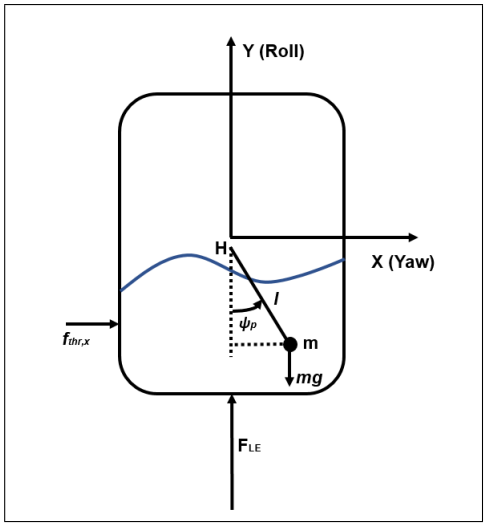


Fig. 2: Sloshing in Roll-Yaw Plane

Consider the propellant tank configuration described in Fig. 2, with forces from engines along the roll axis. The pendulum motion considered here is in two perpendicular planes: roll-yaw and roll-pitch. The slosh dynamics for roll-yaw plane i.e. X-Y plane for a generalized spacecraft configuration with n_0 number of tanks is given by,

$$\begin{aligned} \ddot{\psi}_{p_i} = -\frac{1}{l_i}\Bigg[& -2\omega_y(l_i\dot{\theta}_{p_i}) + \dot{\omega}_y(z_{H_i} - l_i\theta_{p_i}) - \dot{\omega}_z(y_{H_i} - l_i) \\ & + \omega_x\omega_y(y_{H_i} - l_i) + \omega_x\omega_z(z_{H_i} - l_i\theta_{p_i}) \\ & - (\omega_y^2 + \omega_z^2)(x_{H_i} + l_i\psi_{p_i}) + 2\zeta_i\sqrt{\frac{g}{l_i}}l_i\dot{\psi}_{p_i} + g\psi_{p_i} \\ & + \frac{f_x + \sum_{j=1}^{n_0} m_j\psi_{p_j}g}{M_0}\Bigg] \end{aligned} \tag{4}$$

The slosh torque expression for n_0 tanks can be written

as,

$$\tau_{sl} = g \begin{bmatrix} \sum_{i=1}^{n_0} \left(m_i(-\theta_{p_i} y_{Hi} + z_{Hi})\right) \\ \sum_{i=1}^{n_0} \left(m_i(\psi_{p_i} z_{Hi} + \theta_{p_i} x_{Hi})\right) \\ -\sum_{i=1}^{n_0} \left(m_i(x_{Hi} + \psi_{p_i} y_{Hi})\right) \end{bmatrix} \tag{5}$$

Where, g is the lander roll acceleration, m_i is the i^{th} slosh mass and $[x_{Hi}, y_{Hi}, z_{Hi}]^T$ is the hinge location of pendulum and l_i is the pendulum length.
For the Chandrayaan-3 lander, there are two propellant tanks namely, fuel tank and oxidizer tank placed in tandem along the longitudinal axis (roll).

III. Control Stability Assessment

The dynamics parameters of the lander and propellant slosh parameters vary with time. Hence, a short-period dynamics approach (time-slicing approach) is used to analyze the stability. The entire powered descent trajectory is discretized into multiple time-sliced dynamics for which frequency domain techniques are used. Stability analysis is conducted for both the nominal and RCS failure scenarios to ensure robustness in the attitude control loop.

A. State-space Model Derivation

The state space model of the spacecraft attitude dynamics in the presence of propellant sloshing is formulated as,

$$\begin{aligned} \dot{X} &= AX + BU \\ Y &= CX + DU \end{aligned} \tag{6}$$

The state vector $X \in \mathbb{R}^N$ is defined as below,

$$X = \left[\psi\ \phi\ \theta\ \omega_x\ \omega_y\ \omega_z\ \psi_{p_i}\ \theta_{p_i}\ \dot{\psi}_{p_i}\ \dot{\theta}_{p_i}\right]' \tag{7}$$

where, $N = 6 + 4 * n_0$ and subscript 'i' denotes the i^{th} pendulum.
The input vector $U \in \mathbb{R}^6$ is given by,

$$U = [\tau_{RCS}, f_{RCS}]' \tag{8}$$

$Y \in \mathbb{R}^N$ denotes output of the state space model, $C \in \mathbb{R}^{N \times N}$ is the observation matrix and $D \in \mathbb{R}^{N \times 6}$ is a null matrix. τ_{RCS} and f_{RCS} are the RCS torque and force respectively. Details of the derivation of the A and B matrices are given in [3].

B. Linear Stabilty Analysis

The *NGC* loop considered for this study, is shown in Fig.3. The inner loop is the attitude control loop, where the RCS thrusters provide the torque and force to lander dynamics. The lander's angular rate is measured by the gyroscope is fed in the feedback sense to close the attitude control loop. The control reference is provided by the outer loop i.e. the guidance loop. The torque provided by the liquid engines serves as a disturbance torque to the lander in addition to slosh disturbance. The PWPFM is chosen as unity gain in the purview of linear analysis. This whole stability analysis is repeated at regular time intervals within the time zone of interest.

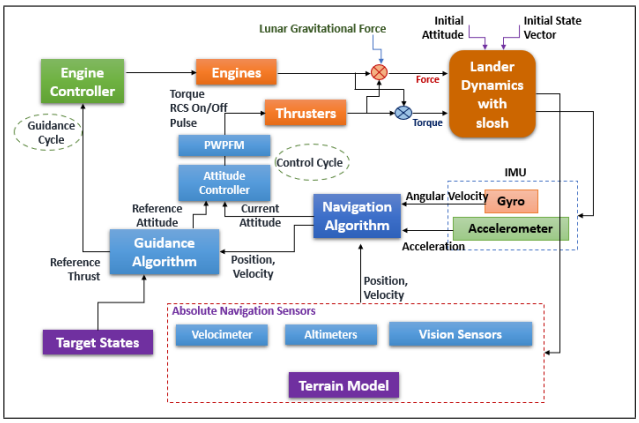


Fig. 3: Chandrayaan-03 Lander NGC Loop

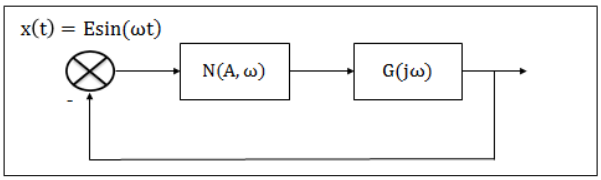


Fig. 4: Closed-loop Block Diagram with Non-linear Element

C. Non-Linear Stability Analysis using Describing Function

The analysis presented in previous sections is extended to include non-linear PWPFM describing function and predicting the system behavior for similar conditions. The describing function analysis is an approximate procedure for analyzing non-linear control problem. In linear analysis, PWPFM is assumed to be a unity gain for generating Nyquist and Bode responses. This aids in evaluating linear system phase margin. When performing analysis for non-linear systems, point of interest gets further extended to predicting limit cycles in the system and stability of limit cycle. Fig.4 describes the close loop linear system with describing function of non-linear element. $N(A, \omega)$ represents the frequency and amplitude response of non-linear element.

For such a scenario, the close loop characteristic equation becomes [6],

$$\begin{aligned} 1 + N(A, \omega) G(j\omega) &= 0 \\ G(j\omega) &= -\frac{1}{N(A, \omega)} \end{aligned} \tag{9}$$

For a non-linear system, stability is computed wrt. $-\frac{1}{N(A,\omega)}$ curve. Followings can be the possible scenario,

- Portion of $-\frac{1}{N(A,\omega)}$ curve lying inside linear curve $G(j\omega)$ indicates unstable operating points.
- Portion of $-\frac{1}{N(A,\omega)}$ lying outside linear curve $G(j\omega)$ indicates stable zone.
- Point at which linear curve $G(j\omega)$ intersect $-\frac{1}{N(A,\omega)}$ is a harmonic balance condition indicating the existence of limit cycle.

Reference [7] gives a detailed description of describing function derivation for various standard non-linearities. In

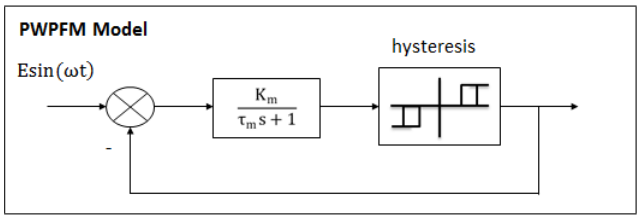


Fig. 5: Architecture of PWPFM Block

general, describing function derivation is performed using Fourier analysis. (10) represents a general expression to evaluate the Fourier coefficient of the first harmonic as,

$$K_{eq} = \frac{i}{\pi E} \int_0^{2\pi} f(Esin\phi) e^{-j\phi}\, d\phi \tag{10}$$

On expanding and expressing in time domain, real and imaginary part can be computed as,

Real part:

$$g(E) = \frac{\omega}{\pi E} \int_0^{T} f(Esin(\omega t)) sin(\omega t)\, dt \tag{11}$$

Imaginary part:

$$b(E) = \frac{j\omega}{\pi E} \int_0^{T} f(Esin(\omega t)) cos(\omega t)\, dt \tag{12}$$

$$-\frac{1}{N(A,\omega)} = -\frac{1}{g(E) + i\, b(E)} \tag{13}$$

[8] provides an analytical expression of describing function assuming only a minimum amplitude requirement to turn on RCS. However, in the actual scenario, the entire amplitude sweep spectrum is required as disturbance varies in several amplitude levels throughout the powered descent till touchdown on the Moon.

Numerically describing function can be computed by sweeping data through non-linear elements and evaluating Fourier integrals as expressed in equation (11)-(13). The non-linear element in the Chandrayaan-3 attitude control loop is in the form of PWPFM, which consists of a low pass filter (defined by k_m and τ_m parameters) and a hysteresis block, cascaded in a feedback architecture shown in Fig. 5.

IV. Results and Discussion

From the mission design perspective, the stability study results for the RCS failure scenario are considered. By designing an appropriate mitigation strategy for such an off-nominal scenario, robustness is guaranteed in the attitude control design of the Chandrayaan-3 lander.

A. Linear Stability Analysis Results

For analysis, the short-period study results for the pitch axis under the RCS failure is included here. Fig.6 shows a family of Nyquist plots for the time-sliced lander dynamics for two RCS failure scenario. $T = 0$ sec corresponds to the beginning of landing on the Moon's surface.

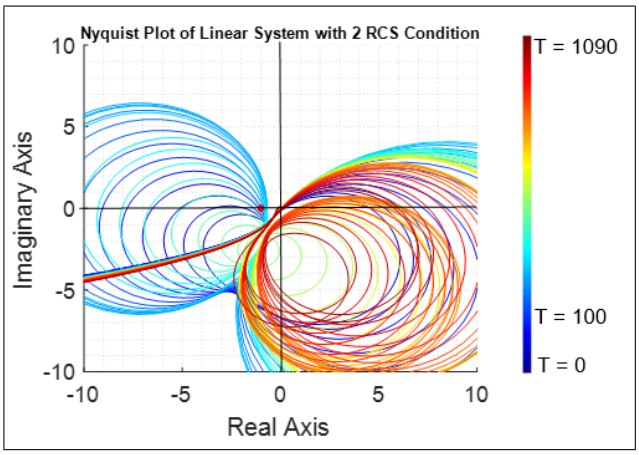


Fig. 6: Nyquist Diagram for 2-RCS Failure Scenario

It can be seen that the phase margins are less for different time instants. This calls for the inclusion of describing function analysis to evaluate the stability of the linearized dynamics with PWPFM non-linearity.

B. Non-linear Stability Analysis Results

Under this approach, both amplitude as well as frequency are swept to generate the describing function profile for the PWPFM. For Chandrayaan-3 lander input amplitude for PWPFM varies from 0.2 to 1.2. The frequency of interest is from 0.01 Hz to 6 Hz. Amplitude sweep data is generated from 0.2 to 1.2 in steps of 0.1. Frequency sweep data is generated from 0.01 Hz to 6 Hz using logarithm sweep.

1) Resolving Initialization Issue in Numerical Apporach: While performing numerical integration, initial condition in general is unknown. In case initialization is done with any arbitrary value, it can add error to numerically computed frequency response. As an example, a low pass filter is subjected to frequency sweep to numerically compute frequency response. It can be seen that if we randomly initialize the initial value (let's say 0), the numerically computed value differs from the analytical value. Fig.7, the red curve (frequency response obtained by numerical approach) clearly shows a difference from the frequency response of analytical form, for example transfer function (low-pass filter). Therefore, we propose the following modified algorithm to numerically compute describing function,

Initialize: $g \leftarrow 0$, $b \leftarrow 0$, $t \leftarrow 0$
while $t < 2T$ **do**
  if $t < T$ **then**
    $g \leftarrow \frac{\omega}{\pi E} \int_0^T f(Esin(\omega t)) sin(\omega t)\, dt$
    $b \leftarrow \frac{j\omega}{\pi E} \int_0^T f(Esin(\omega t)) cos(\omega t)\, dt$
  else
    $g \leftarrow g + \frac{\omega}{\pi E} \int_0^T f(Esin(\omega t)) sin(\omega t)\, dt$
    $b \leftarrow b\frac{j\omega}{\pi E} \int_0^T f(Esin(\omega t)) cos(\omega t)\, dt$
  end if
end while

g is the real part and b is the imaginary part.
In Fig.7, the black curve represents the describing function

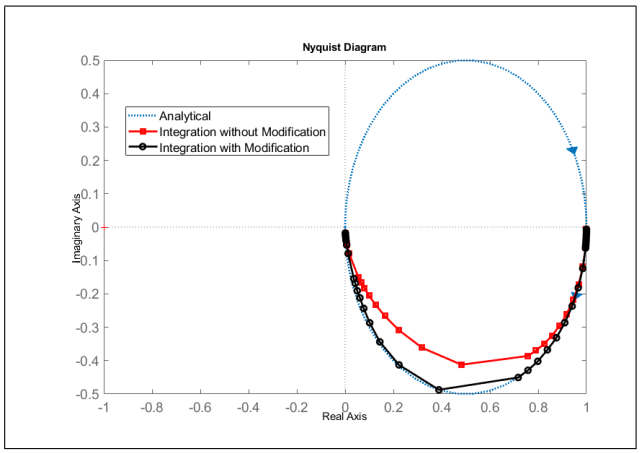


Fig. 7: Analytical and Numerical Approach

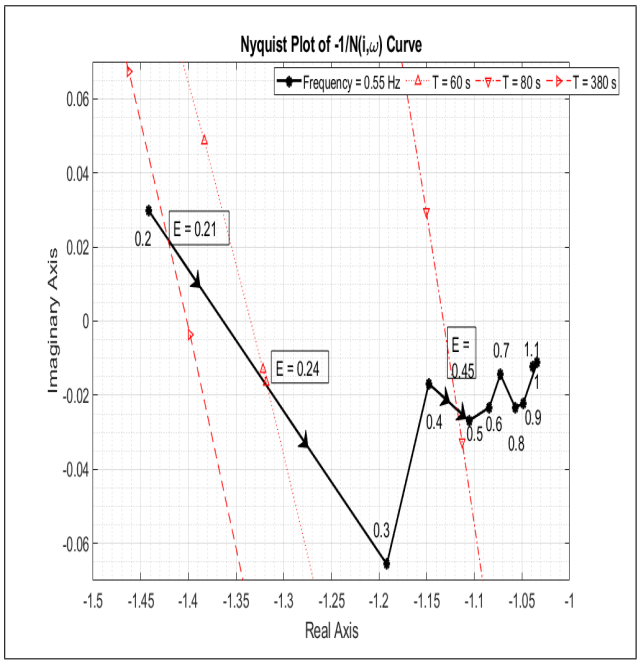


Fig. 8: Describing function of PWPFM Block

with the modified algorithm, which matches with the frequency response of the analytical form.

2) Non-linear Stability Analysis with PWPFM: Fig.8 illustrates the numerically derived describing function (with proposed computational modification) of PWPFM. Typically slosh frequency for the Chandrayaan-3 lander varied from 0.5 Hz to 0.6 Hz. Hence to evaluate the existence of limit cycle, 0.55 Hz frequency for varying amplitude is chosen.

For the two RCS failure condition, the Nyquist curve very closely passes through the $-1 + j0$ point. To predict limit cycle, $G(j\omega)$ is plotted along with $-\frac{1}{N(A,\omega)}$. The following can be noted from Fig.9,

- First set of $G(j\omega)$ curves (plotted in blue color) neither cut nor encircle the $-\frac{1}{N(A,\omega)}$ curve. For this set of $G(j\omega)$ curves there will not be any limit cycle corresponding to slosh frequency ($F = 0.55$ Hz). These curves also indicate the system is stable wrt. slosh oscillation for those specified time stampings.
- Second set of $G(j\omega)$ curves (plotted in green color) cuts the $-\frac{1}{N(A,\omega)}$ curve. For this set of $G(j\omega)$ curves, there will limit cycle corresponding to slosh frequency ($F = 0.55$ Hz). Amplitude of limit cycle for these curves are given in Table II. The stability of these limit cycles are discussed in the next section.
- Third set of $G(j\omega)$ curves (plotted in red color) completely encircle the $-\frac{1}{N(A,\omega)}$ curve. Complete encirclement indicates system instability. For these time instances, the amplitude of oscillation is indeed unbounded.

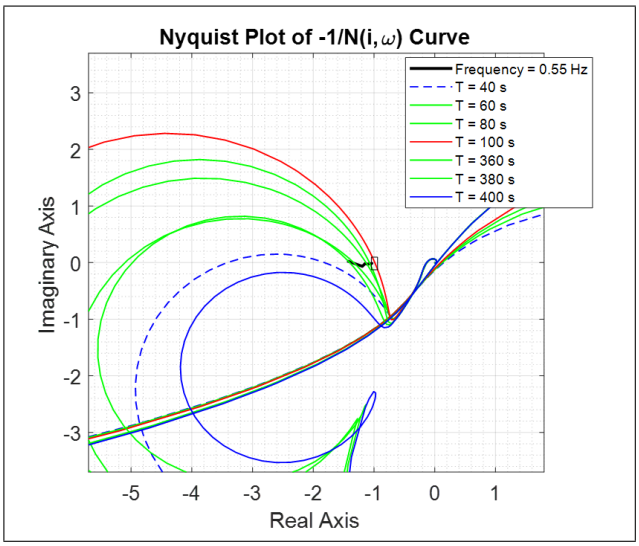


Fig. 9: Non-linear Stability Analysis: 2-RCS Failure Case

The summary of the non-linear stability analysis is documented in Table I.

TABLE I: Summary of Non-linear Stability Analysis

Stability Nature	Time Zone
Stable zone	0 s to 40 s
Limit cycle	40 s to 100 s
Unstable zone	100 s to 340 s

3) Stability of Limit Cycle: A total of four linear $G(j\omega)$ curves cut the describing function curve as seen in Fig.8. The stability of these limit cycles is obtained through the extended Nyquist criteria which is described in [7]. Based on the *extended Nyquist criteria*, the stability of these limit cycles is derived and tabulated in Table II.

4) Reduction in Phase Margins: For linear systems with nonlinear elements, phase margins are described for each operating amplitude [4]. Thus, these margins are computed with respect to each operating amplitude and compared against the linear system. Fig.10 represents the same.

TABLE II: Summary of Limit Cycle Amplitude and Stability

Time	Amplitude	Stability	Remark
60 s	$E = 0.21$	Stable limit cycle	This amplitude is corresponding to PWPFM input
80 s	$E = 0.45$	Stable limit cycle	
360 s	$E = 0.70$	Stable limit cycle	
380 s	$E = 0.24$	Stable limit cycle	

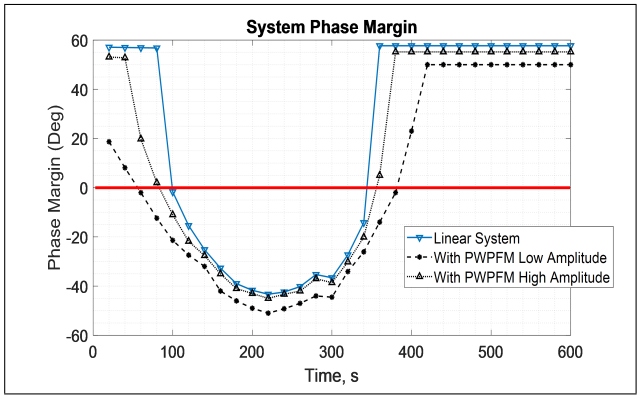


Fig. 10: System Phase Margin

C. Time Domain Comparison

For the Chandrayaan-3, a high-fidelity computer simulation software was developed that emulates the actual performance of realistic sensor and actuator models, onboard logic processing delays, and real-time controls. In this simulator, the control system designed for the lander was implemented and simulation was done for both nominal and RCS failure conditions. Fig.11 represents the simulation result of spacecraft body rate and slosh pendulum angles under two RCS failure scenario. The oscillation observed in the rate plot as well as in the pendulum angle between 400 sec and 600 sec of powered descent is the unstable slosh oscillation inside tanks. This behavior in time domain simulation exactly correlates with the frequency domain analysis carried out with and without PWPFM. To handle such possible instability in case of RCS failure, controller *gain scheduling* is considered along with the introduction of *mechanical baffles* inside the propellant tanks.

V. CONCLUSIONS

In this paper, we propose a novel method to numerically compute the describing function for any general non-linearity. The method addresses issues related to the integration constant's initialization, ensuring accurate results. The accuracy was demonstrated using a simple low-pass filter. The proposed method was used to derive the describing function for PWPFM non-linearity in the attitude control loop of the Chandrayaan-3 attitude control system. Prediction of limit cycles was done based on Nyquist criteria, and stability was derived using the extended Nyquist criteria. Correlation of frequency domain linear and non-linear stability analysis was conducted for high-fidelity time-domain computer simulation, demonstrating the efficiency of the proposed method.

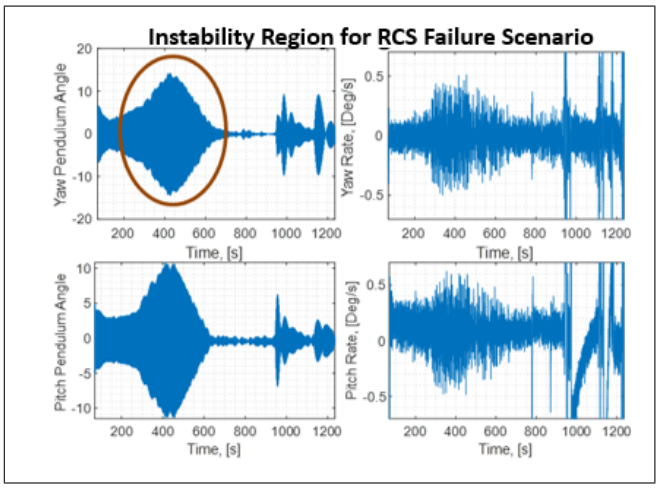


Fig. 11: Time Domain Results: 2-RCS Failure Case

ACKNOWLEDGMENT

The authors of this paper would like to convey gratitude to Dr. MS Siva Group Director CDDG, Dr. Ravi Kumar L Group Director MSG, Dr. Veeramuthuvel P Project Director Chandrayaan-3, U. R. Rao Satellite Centre, Bengaluru, for their support and valuable suggestions during this work. Last but not least, a special vote of thanks to the excellent review committee at ISRO for the Chandrayaan mission series who reviewed this work and provided valuable feedbacks regarding this research.

REFERENCES

[1] M. J. Sidi, Spacecraft dynamics and control: a practical engineering approach, Vol. 7. Cambridge university press, 1997.

[2] A. L. Greensite, Analysis and design of space vehicle flight control systems. Volume VII-Attitude control during launch, tech. rep., 1967.

[3] Nivriti Priyadarshini, Debajyoti Chakrabarti, and Yajur Kumar Modelling of Propellant Slosh Dynamics and Its Application in Control Stability Study of Lunar Landing Mission. In AAS/Astrodynamics Specialist Conference 2022.

[4] J.E. Gibson, Nonlinear Automatic Control. New York: McGraw-Hill, 1963.

[5] Schwartz C, Gran R. Describing function analysis using MATLAB and Simulink. IEEE Control Systems Magazine. 2001 Aug;21(4):19-26.

[6] Agrawal BN, Mcclelland RS, Song G. Attitude control of flexible spacecraft using pulse-width pulse-frequency modulated thrusters. Space Technology. 1997;1(17):15-34.

[7] J-J.E. Slotine and W. Li, Applied Nonlinear Control. Englewood Cliffs, NJ: Prentice-Hall, 1991

[8] Wang X, Wang D, Zhu S, Poh EK. Fractional describing function analysis of PWPF modulator. Mathematical Problems in Engineering. 2013;2013(1):287040.